

Geometrically Nonlinear Free Vibration Analysis of Cylindrical Shells Using high Order Shear Deformation Theory-A Finite Element Approach

Dr. Nabil Hassan Hadi * & Kayser Aziz Ameen *

Received on :5/4/2011

Accepted on: 20/6/2011

Abstract

A nonlinear finite element model for geometrically large amplitude free vibration analysis of laminated composite shallow cylindrical shell panel is presented using high order shear deformation theory (HSDT). The nonlinearity is introduced in the Green – Lagrange sense. The effects of different orthotropic ratios, thickness ratio, curvature ratio and boundary condition are study also frequency ratio (nonlinear frequency to linear frequency) of cylindrical shell are determined as function of shell amplitude ratio.

Keywords: High order shear deformation, Shell, Free vibration, Nonlinear Finite element Method.

تحليل الاهتزازات الحرة للأشكال الهندسية اللاخطية للرقائق الاسطوانية وباستعمال نظريات القص عالية الرتبة – طريقة العناصر المحددة

الخلاصة

طريقة العناصر المحددة اللاخطية لتحليل الأشكال الهندسية ذات السعات الاهتزازية الحرة العالية لرقائق الاسطوانية المركبة المتعددة السطحية تم تقديمها باستخدام صيغة نظرية القص عالية الرتبة. تم اعتماد اللاخطية في اتجاه الكرين لاكرانج. تم دراسة تأثير تغيير نسبة الخواص المتعامدة للمواد المركبة، نسبة سمك الاسطوانة، نسبة التقوس والشروط الحدية وكذلك تم دراسة نسبة التردد (التردد الخطي الى التردد اللاخطي) لرقائق الاسطوانية وتم حسابه نسبة الى نسبة السعات.

Notations

- α, β, ζ : Curvilinear coordinate axes
- $\bar{u}, \bar{v}, \bar{w}$: Displacement along the
 α, β, ζ
 coordinate
- u, v, w : The displacements of a
 point on
 the mid-plane
- R_1, R_2 : Radii of curvature of shell
 (m)
- ϕ_1, ϕ_2 : The rotations with respect
 α and
 β direction respectively
- $\psi_1, \psi_2, \theta_1, \theta_2$: High order terms of
 Taylor
 series expansion
- $\{\epsilon_L\}, \{\epsilon_{NL}\}$: Linear and nonlinear
 strain
 vectors
- $[Q]$: Transferred reduced elastic
 constant
- E : Young's modulus (GPa)
- G : Shear modulus (GPa)
- ν : Poisson's ratio
- W_{max} : Maximum deflection (m)
- h : thickness of laminated
 shallow
 cylindrical (m)
- ω_{nL} : Linear natural frequency
 (rad/sec)
- ω_{NL} : Nonlinear natural frequency
 (rad/sec)
- ω_{NL}/ω_{nL} : Frequency ratio
- κ : Damage ratio for linear and
 nonlinear
 respectively
 $(\omega_{int act} - \omega_{delamination}) / \omega_{int act}$

Introduction

Laminated composite structures are playing an imperative role in different fields of our life like aerospace, automotive, naval, mechanical and civil industries over the past three decades. The main reasons for this trend are outstanding mechanical properties of composite, such as high strength to weight ratio, excellent corrosion resistance and very good fatigue characteristics. Its ability to allow the structural properties to be tailored according to requirements adds to the versatility of composite for sensitivity application. It can be seen from the literature that the amount of work carried out on the vibration characteristics of isotropic plates, shells and composite laminates are exhaustive. Some of the important contributions are briefly mentioned here.

A considerable literature is available on the nonlinear free vibration analysis of the laminated composite shells in Von-Karman sense with and without taking into account the transverse shear effects. **Shin DK 1997**, analyzed the large amplitude vibration of symmetrically laminated moderately thick shallow doubly curved open shells with simply supported sides, considering the first order shear deformation theory and nonlinearity in Von-Karman sense. They obtained the governing equations using the Galerkin approximation and solved them by a fourth order Runge Kutta time integration procedure. **Reddy and Chao 1981** used the solution of finite element methods to determine the bending deflection, stress, and natural frequency for large deflection theory (Von Karman's), including

transverse shear, governing moderately thick, laminated anisotropic composite rectangular plate subjected to various loading and edge condition was presented. The Navier type exact solution are presented by **Reddy and Liu 1985** used the high order shear deformation theory of elastic shells is developed for shells laminated of orthotropic layers. The theory is a modification of the Sanders theory and accounts for parabolic distribution of the transverse shear strains through thickness of the shell and tangential stress free boundary conditions on the boundary surfaces of the shell. **Shiau and Wu 1991** can obtain A high precision based on a simplified high order shear deformation plate theory and used the finite element formulation (72 degree of freedom and triangular element) to determine the natural frequency of laminated plate for deferent type of material and number of layers. The **Malekzadeh 2007** studied the effect of different parameters on the convergence and accuracy of natural vibration of the method a differential quadrature for large amplitude free vibration analysis of laminated composite skew plates, the governing equations are based on the thin plate theory (classical linear theory) and geometrical nonlinearity is modeled using Green's strain in conjunction with Von Karman assumption. On the other hand The **Ganapathi, etal. 2009** investigated the free vibration characteristics of simply supported anisotropic composite laminates using analytical approach the formulation is based on the first order shear deformation theory, the governing equation are obtained

using energy method. **Dongwei and Christian 2004** An analytical solution to the free vibration of composite beams with two non overlapping delaminations is presented, the Euler Bernoulli beams used the delaminations as their boundaries, the continuity and the equilibrium conditions are satisfied between adjoining beams. **Wang and Dong 2005** used the energy method to study hygothermal effects on local buckling for different delaminated shapes near the surface of cylindrical laminated shells, the effect of non-linear obtained by considered transverse displacements of sub laminate shells and the young's modulus, thermal and humidity expansion coefficients of material are treaded as functions of temperature. **Yang and Fu 2006** discuss the effects of delamination sizes, depths, boundary conditions, the material properties and the laminate stacking sequences on delamination growth for beams, and used classical theory for cylindrical shells. In this work, an effort has been made to predict such a complex problem. All the higher order terms of curvature have been included in the formulation. A nonlinear finite element method is proposed for this nonlinear model. The nonlinear fundamental frequencies are obtained for different orthotropicity ratios the stacking sequences, the thickness ratios, the amplitude ratios and boundary condition.

Mathematical Model

Displacement field

A shell of length a , width b and thickness h is composed of N number of orthotropic layers of uniform thickness. The (α, β, ζ) it was

curvature coordinate . The following displacement field for the laminated shell based on the HSDT is considered to derive the mathematical model.

$$\left. \begin{aligned} \bar{u}(\alpha, \beta, \zeta, t) &= u + \zeta\phi_1 + \zeta^2\psi_1 + \zeta^3\theta_1 \\ \bar{v}(\alpha, \beta, \zeta, t) &= v + \zeta\phi_2 + \zeta^2\psi_2 + \zeta^3\theta_2 \\ \bar{w}(\alpha, \beta, t) &= w \end{aligned} \right\} \quad (1)$$

Where t is the time, $(\bar{u}, \bar{v}, \bar{w})$ are the displacement along the (α, β, ζ) coordinates, (u, v, w) are the displacements of a point on the mid-plane and ϕ_1 and ϕ_2 are the rotations at $(\zeta = 0)$ of normal to the mid-plane respect to the α and β -axes, respectively, $\psi_1, \psi_2, \theta_1, \theta_2$ are high order terms of Toyler series expansion defined at the mid-plane.

Strain –displacement relation

The nonlinear Green Lagrange stain displacement relation for the laminated shell can be expressed as follows.

Substituting equation (1) in equation (2) (in Appendix A) the strain – displacement relation of the laminated shell is further expressed as shown in equation (3) in Appendix (A).

The value of individual terms of above equation which are provided in reference [Nabil Hassan Hadi and Kayser Aziz Ameen].Hence the above equation can be rearrangement as shown in Appendix (A) equation (4).

Stress - strain relations

In the analysis of composite laminated materials, the assumption of plane stress is usually used for each layer. This mainly because fiber reinforced material are utilized in beam, plate, cylinders, spherical and other structural shapes which have at least one characteristic geometric dimension in an order of magnitude less than the other two dimensions. In this case the stress components $(\sigma_3, \tau_{23}, \tau_{13})$ are set to zero. Then The strain displacement relations, for any general k^{th} orthotropic composite lamina with an arbitrary fiber orientation angle with reference to the coordinate axes (α, β, ζ) is written as in equation (5) in Appendix (A).

Strain energy of the laminate

Energy and variational principle offered great simplification to many derivations of fundamental equations in elasticity. Also have been used to introduce and implement approximation techniques for structural systems. Strain energy is defined as the work done by the internal stresses which caused elongation or shear strains. The strain energy of the plate can be expressed as :

$$U = \frac{1}{2} \int_V \{\epsilon\}_i^T \cdot \{\sigma_i\} dV \quad (6)$$

By substituting the strains from equation (2) and stresses from equation (5) (in Appendix A) into equation (6) the strain energy can be expressed in equation (7) in Appendix (A).

Kinetic energy of the vibrating shell

The kinetic energy expression of a vibrated shell can be expressed as

$$T = \frac{1}{2} \int_V \rho \{\dot{\bar{\delta}}\}^T \{\dot{\bar{\delta}}\} dV \tag{8}$$

Where, ρ and $\bar{\delta}$ are the density, displacement vector which differentia the first order of displacement with respect to time, respectively. The global displacement vector can be expressed in appendix A.

Then the kinetic energy for ‘N’ number of orthotropic layered composite plate obtained by substituting the equation (9) into equation (8) obtain.

$$T = \frac{1}{2} \int_A \left(\sum_{k=1}^N \int_{\zeta_{k-1}}^{\zeta_k} \{\dot{\delta}\}^T [f]^T \rho^k [f] \{\dot{\delta}\} d\zeta \right) dA \tag{10}$$

$$T = \frac{1}{2} \int_A \{\dot{\delta}\}^T [m] \{\dot{\delta}\} dA$$

Where,

$[m] = \sum_{k=1}^N \int_{\zeta_{k-1}}^{\zeta_k} ([f]^T \rho^k [f]) d\zeta$ is the inertia matrix.

Solution Technique

In the case of the shell element the external and inner face are curved, and each point on the surface are given by Cartesian coordinate as shown in the Figure (1).

Let the (α, β) be two curvilinear coordinate in the middle plane of the shell and (ζ) a linear coordinate in the thickness direction. If further we assume that $(\alpha, \beta$ and $\zeta)$ vary between (-1 and 1) on the respective faces of the element we can write a relationship between the Cartesian coordinate of any point of the shell and the curvilinear coordinates in the form

It is convenient to rewrite relationship (11) in a form specified by the vector connecting the upper and lower points (i.e a vector of length equal to the shell thickness) and the mid surface coordinates.

$$\begin{Bmatrix} x \\ y \\ z \end{Bmatrix} = \sum N_i(\alpha, \beta) \begin{Bmatrix} x_i \\ y_i \\ z_i \end{Bmatrix}_{mid} + \sum N_i(\alpha, \beta) \frac{\zeta}{2} \vec{V}_{3i}$$

Where :-

$$V_{3i} = \begin{Bmatrix} x_i \\ y_i \\ z_i \end{Bmatrix}_{Top} - \begin{Bmatrix} x_i \\ y_i \\ z_i \end{Bmatrix}_{Bottom}$$

The displacement vector can be conceded to the form by employing the FEM

$$\{\mathcal{D}\} = [N_i] \{\delta_i\} \tag{12}$$

Where :

$$\{\delta_i\} = [u_i \ v_i \ w_i \ \phi_1 \ \phi_2 \ \psi_1 \ \psi_2 \ \theta_1 \ \theta_2]^T$$

The equations of strain for linear and nonlinear are studied of large deflections, as in equation (4) and nonlinear displacement in equation (1), when substituted into equation (7), the strain energy can be written as in appendix A.

The value of individual terms of $[B_{NL}]$ which are provided in reference [Nabil Hassan Hadi and Kayser Aziz Ameen].

The final form of governing equation for the nonlinear free vibration laminated plate panel is obtained by using Hamilton’s principle. It can be viewed and axiom, from which other axioms like Newton’s second law, Let us define the potential energy to be

($\Pi = U - W$), which U is the strain energy and W is the work done and the Lagrangian as the function L where ($L = (T - U + W)$).

Hamilton's principle states that the actual displacement that the body actually goes through from instant (t_1) to instant (t_2) out of many possible paths, is that which achieves an extremum of the line integral of the Lagrangian function. This is achieved if the variation of the time integral of the Lagrangian is set to zero:

$$\delta \int_{t_1}^{t_2} L dt = 0 \quad (14)$$

Hamilton's principle can be used to find the compatible set of equations of motion and boundary conditions for given stresses and strains. This is done by substituting the equations for strain energy equation (13) and kinetic energy equation (10) into the equation (14), performing the integration by parts, and setting the coefficients of the displacement variations (also called virtual displacement) equal to zero. The Lagrangian becomes (Marco, 2008).

$$[M] \{\dot{\delta}\} + ([K_L] + [K_{NL}]) \{\delta\} = 0 \quad (15)$$

Where $\{\delta\}$ is the displacement vector, $[M]$, $[K_L]$ and $[K_{NL}]$ are the global mass matrix and global linear stiffness matrix and nonlinear stiffness matrix that depend on the displacement vector respectively.

Numerical results and discussion

A nonlinear finite element code is developed in MATLAB 8.0 using the present displacement field shell model in Green-Lagrange sense in the framework of the HSDT. The validation and accuracy of the present algorithm are examined by comparing the results with those available in the literature. The effect of different combinations of the material orthotropy, amplitude ratio (W_{max}/h).

The following sets of boundary conditions are used for the present analyses

a-Simply support boundary conditions (S):

$$v = w = \phi_2 = \psi_2 = \theta_2 = 0 \quad \text{at } x=0,a$$

$$u = w = \phi_1 = \psi_1 = \theta_1 = 0 \quad \text{at } y=0,b$$

b-Clamped supported boundary condition (C)

$$u = v = w = \phi_1 = \phi_2 = \psi_1 = \psi_2 = \theta_1 = \theta_2 = 0 \quad \text{at } x=0,a$$

$$u = v = w = \phi_1 = \phi_2 = \psi_1 = \psi_2 = \theta_1 = \theta_2 = 0 \quad \text{at } y=0,b$$

A convergence of the mathematical model developed for laminated shell is presented Figure (2). are shown the nondimensional fundamental

$$\text{frequency } (\bar{\omega} = \omega \left(\frac{a^2}{h}\right) \sqrt{\left(\frac{\rho}{E_2}\right)}),$$

against mesh division respectively for simply support boundary condition and for different stacking sequences, The results are plotted using the material properties ($E_1=181 \text{ GPa}$, $E_2=7.17 \text{ GPa}$, $G_{23}=6.71 \text{ GPa}$, $\nu_{12}=0.28$, and the geometry parameters are $a/b=1$, $a/h=10$). From the figures shown that the

convergence is a (5X5) mesh, then it's used to compute the results throughout the study.

In order to show the validation of the present intact model, simply supported square laminated cylindrical shell panels of symmetric angle ply lamination $[\pm 45^\circ]_s$ are studied with the geometry cylindrical shell ($a/b=1$, $a/h=10$ and $R/h=100$). The composite properties ($E_1=181$ GPa, $E_2=10.3$ GPa, $G_{12}=7.17$ GPa, $G_{23}=6.21$ GPa and $\nu_{12}=0.28$) are used for the computation of the result. The results in terms of the frequency ratio $\left(\frac{\omega_{NL}}{\omega_L}\right)$, ie., ratio of the nonlinear frequency to linear frequency are computed for different amplitude ratios (W_{max}/h), (to find this ratio first when the maximum deflection (W_{max}) equal to the thickness ($W_{max}/h=1$) such as $h=5$ mm then the $W_{max}=5$ mm after that we increase the ratio ($h=5 \times 0.5, 8, 1.1, 2, 1.5$ which $0.5, \dots, 1.5$ were the ratio) then at each ratio find the natural frequency when consider the Von-Karman and with out consider). The present results and their differences with the existing result (Shin DK) are depicted in Table (1). The differences are more pronounced because the present study deals with all the higher order terms of Green-Lagrange strains in the framework of the high shear order theory. Due to this, the stiffness matrix becomes more flexure and approaches towards the more general case, ie., Green-Lagrange. However, the published results (Shin DK) have been obtained using the Von-Karman strains in the framework of the first shear order theory.

The effect of material orthotropy on the frequency ratio of the

nonlinear free vibration of square laminated cylindrical shell are studied for four different modular ratio ($E_1/E_2 = 3, 5, 10$ and 15) with other parameters such as ($G_{12}/E_2=0.6$, $G_{23}/E_2=0.5$, $\nu_{12}=0.25$, $a/b=1$, $a/h=10$, $R/a=5$) for all sides simply supported boundary condition (SSSS). The results of the linear fundamental frequency increase with increase in modular ratio as shown in figure (3) and the reduction in natural frequency when considering the nonlinearity (13.67% for $[0/90/0/90]_s$, 16.62% for $[45/-45/45/-45]_s$ and 17.11% for $[0/45/-45/90]_s$). The frequency ratio decreases with increase in modular ratio and diverge in some results because the present work used in the framework of the high order shear theory and geometrical nonlinearity modeled using Green's strain. as shown in Table (2).

The effect of the thickness ratio ($a/h=10, 20, 50$ and 100) on the frequency ratio of a cylindrical shell is analyzed. The material properties are ($E_1/E_2 = 15$, $G_{12}/E_2=0.6$, $G_{23}/E_2=0.5$, $\nu_{12}=0.25$, $a/b=1$, $R/a=5$) for all sides simply supported boundary condition (SSSS). The results are depicted in Table (3) and Figure (4), the frequency ratio decreases with increase in the thickness ratio and the non-dimensional linear frequency increase with increase the thickness ratio.

The variation of the frequency ratio for unlike stacking sequences, the curvature ratio ($R/a=10, 20, 50$ and 100) and different amplitude ratio of cylindrical shell is shown in Table (4) and in Figure (5). The results are using the material

properties and other parameters such as ($E_1/E_2 = 15$, $G_{12}/E_2=0.6$, $G_{23}/E_2=0.5$, $\nu_{12}=0.25$, $a/b=1$, $a/h=10$). From the table it is clear that as the curvature ratio increases the frequency ratio decreases. The linear non-dimensional frequency is also computed and presented in Figure (4) which noted that decreasing in linear non-dimensional frequency with increasing the curvature ratio. The results also shows that few diverge because of severe nonlinearity.

The effect of number of layers and the amplitude ratio on the frequency ratio are summarized in Table (5) and Figure (6) for lamination scheme ([0/90/0], [0/90/0/90/0], [0/90/0/90]s and [0/90/0/90/0/90]s). The results are using the material properties and other parameters such as ($E_1/E_2 = 15$, $G_{12}/E_2=0.6$, $G_{23}/E_2=0.5$, $\nu_{12}=0.25$, $a/b=1$, $a/h=10$, $R/a=10$) for all sides simply supported boundary condition. The frequency ratio decreases with increase in number of layers and the non-dimensional linear frequency increase with increase in number of layers.

The variation of the frequency ratio for different support conditions and the amplitude ratios are analyze for different lamination schemes. The results are shown in Table (6) and Figure (7). In this part of the study the effects of three different support conditions are examined on the frequency ratio such as all sides simply support (SSSS), all sides clamped (CCCC) and two sides simply support and two side clamped (SCSC). The material properties and other parameters such as ($E_1/E_2 = 15$, $G_{12}/E_2=0.6$, $G_{23}/E_2=0.5$, $\nu_{12}=0.25$, $a/b=1$, $a/h=10$, $R/a=10$) used for the computation of the result. The

frequency ratio decrease in amplitude ratio increase for all type of boundary condition.

Conclusions

The geometrically nonlinear free vibration analysis of composite plate with and without containing the delamination is investigated using nonlinear finite element method in the framework of a higher order shear deformation theory in Green-Lagrange sense. The frequency amplitude relations for the nonlinear free vibrated plate are computed using eigenvalue formulation and are solved employing a direct iterative procedure. Based on the numerical results the following conclusions are drawn.

- The validation shows the necessities of taking into account full nonlinearity.
- The finite element model proposed can be predicted accurately the dynamic behaviors of a laminated composite plate with internal delamination at arbitrary location. Hence the discrepancy of the results was (15.8022 % with considering the nonlinearity).
- Local internal delamination has slight effect on the natural frequencies of the laminated composite plate although the extent of the natural frequency variation increases with both the delamination dimension and the order of the natural frequency.

References

- [1]Shin DK., "Large Amplitude Vibration Behavior of Doubly Curved Shallow Shells With Simply Supported Edges",

- Computer Structure, Vol. (1), No. (62), pp. 35-49, 1997.
- [2]Reddy J. N. and Chao W. C., “*Large Deflection and Large Amplitude Free Vibrations of Laminated Composite Material Plates*”, Journal of Computers & Structures, Vol. 13, pp. 341-347, April 1981.
- [3]Reddy J.N. and Liu C. F., “*A High Order Shear Deformation Theory of Laminated Elastic Shells*”, Int. Journal Engineering Science, Vol. 23, No. 3, pp. 319-330, 1985.
- [4]Shiau L. C. and Wu T. Y., “*A High Precision High order Triangular Element for Free Vibration of General Laminated Plates*”, Journal of Sound and Vibration, Vol. 161, No. 2, pp. 265-279, October 1991.
- [5]Malekzadeh P., “*A differential Quadrature Nonlinear Free Vibration Analysis of Laminated Composite Skew Thin Plates*”, Journal of Thin Wall Structures, Vol. (45), pp. 237-250, January 2007.
- [6] Ganapathi M., Amit Kalyani, Bhaskar Mondal, Prakash T., “*Free Vibration Analysis of Simply Supported Composite Laminated Panels*”, Journal of Composite Structures, Vol. (90), pp. 100-103, February 2009.
- [7]Dongwei Shu and Christian N. Della, “*Free Vibration Analysis of Composite Beams With Two Non-Overlapping Delaminations*”, Journal of International Mechanical Sciences, Vol. (46), pp. 509-526, May 2004.
- [8]Wang X. and Dong K., “*Local Buckling for Triangular And Lemniscate Delaminations Near The Surface of Laminated Cylindrical Shells Under Hygrothermal Effects*”, Journal of Composite Structures, Vol. (79), pp. 67-75, December 2005.
- [9]Yang and Fu, “*Flexural Vibrations of Beams With Delamination*”, Journal of Sound Vibration, No. (125), pp. 441-461,2006.
- [10]Nabil Hassan Hadi and Kayser Aziz Ameen, “*Nonlinear Free Vibration Of Cylindrical Shells With Delamination Using High Order Shear Deformation Theory :- A Finite Element Approach*”, American journal of Scientific and industrial Research, Vol. 2, Issue No. 2, pp. 251-277,2011.

Table (1) Comparison of frequency ratio $\left(\frac{\omega_{NL}}{\omega_L}\right)$ of square angle $[\pm 45^\circ]_s$ laminated cylindrical shell for SSSS boundary condition

W_{max}/h	Shin DK	Present Work
0.2	1.0281	1.166719135
0.4	1.0957	1.019832623
0.6	1.2023	0.936271035
0.8	1.30368	0.99989171
average error (%)=16.45904		

Table (2) Effect of material orthotropy on nonlinear free vibration of laminated cylindrical shell

0/90/0/90/0/90/0/90				
W_{max}/h	E_1/E_2			
	3	5	10	15
0.5	1.672687559	1.427193335	1.175672797	1.117434145
1	1.553800821	1.301946392	1.062937543	1.043722707
1.5	1.515533463	1.272510906	1.040317693	1.029731976
2	1.501928192	1.26207732	1.032320108	1.024763747
45/-45/45/-45/45/-45/45/-45				
W_{max}/h	E_1/E_2			
	3	5	10	15
0.5	1.674726071	1.410753328	1.099153078	0.953255327
1	1.549655278	1.310078295	1.032805693	0.896334061
1.5	1.513669461	1.29077769	1.020217106	0.885552051
2	1.500864133	1.283835712	1.015702084	0.881702682
0/45/-45/90/0/45/-45/90				
W_{max}/h	E_1/E_2			
	3	5	10	15
0.5	1.672687557	1.415017862	1.083540855	0.949228308
1	1.553799051	1.300610542	1.013675441	0.88141936
1.5	1.515533463	1.278444234	1.000400976	0.868474041
2	1.501928192	1.270528361	0.995657977	0.863880487

Table (3) Variation of frequency of laminated cylindrical shell for different thickness ratio

[0/90/0/90/0/90/0/90]				
Thickness ratio (a/h)				
W_{max}/h	10	20	50	100
0.5	0.995163672	0.995989891	0.945902172	0.968499531
1	0.982261225	0.98253814	0.93691108	0.961663992
1.5	0.965647406	0.965346216	0.924716796	0.952000054
2	0.947767427	0.950245124	0.91104925	0.940762715
[45/-45/45/-45/45/-45/45/-45]				
Thickness ratio (a/h)				
W_{max}/h	10	20	50	100
0.5	1.211084329	1.186263118	0.870931957	0.774350296
1	1.19328851	1.166592484	0.860495641	0.768023597
1.5	1.171269981	1.142842444	0.847063366	0.759333344
2	1.148072284	1.118127394	0.832583126	0.749516914
[0/45/-45/90/0/45/-45/90]				
Thickness ratio (a/h)				
W_{max}/h	10	20	50	100
0.5	0.994880536	0.994910849	0.851931981	1.003496992
1	0.981248996	0.982588223	0.84295392	0.995971013
1.5	0.964004368	0.964191207	0.831040971	0.985446734
2	0.945633912	0.944770372	0.817932604	0.97336475

Table (4) Frequency ratios of laminated cylindrical shell for different curvature ratios, lamination schemes and amplitude ratios.

[0/90/0/90/0/90/0/90]				
R/a				
W_{max}/h	10	20	50	100
0.5	0.995163672	0.995989891	0.945902172	0.968499531
1	0.982261225	0.98253814	0.93691108	0.961663992
1.5	0.965647406	0.965346216	0.924716796	0.952000054
2	0.947767427	0.950245124	0.91104925	0.940762715
[45/-45/45/-45/45/-45/45/-45]				
R/a				
W_{max}/h	10	20	50	100
0.5	1.211084329	1.186263118	0.870931957	0.774350296
1	1.19328851	1.166592484	0.860495641	0.768023597
1.5	1.171269981	1.142842444	0.847063366	0.759333344
2	1.148072284	1.118127394	0.832583126	0.749516914
[0/45/-45/90/0/45/-45/90]				
R/a				
W_{max}/h	10	20	50	100

0.5	0.994880536	0.994910849	0.851931981	1.003496992
1	0.981248996	0.982588223	0.84295392	0.995971013
1.5	0.964004368	0.964191207	0.831040971	0.985446734
2	0.945633912	0.944770372	0.817932604	0.97336475

Table (5) Effect of number of layers on the frequency ratio and amplitude ratio

W_{max}/h	[0/90/0]	[0/90/0/90/0]	[0/90/0/90]s	[0/90/0/90/0/90]s
	Amplitude Ratio			
0.5	0.994126671	0.993479344	0.995163672	0.994617709
1	0.979183295	0.977133428	0.982261225	0.98058019
1.5	0.960576377	0.957068515	0.965647406	0.962787474
2	0.940910088	0.936105529	0.947767427	0.943848581

Table (6) Effect of various boundary conditions on frequency ratios of cylindrical

W_{max}/h	[0/90/0/90/0/90/0/90]		
	Boundary Condition		
	SSSS	SCSC	CCCC
0.5	1.117122228	1.144280709	1.247976244
1	1.117122228	1.03659193	1.058801939
1.5	1.029696605	1.015228814	1.007639366
2	1.024744024	1.00768562	0.98543487
W_{max}/h	[45/-45/45/-45/45/-45/45/-45]		
	Boundary Condition		
	SSSS	SCSC	CCCC
0.5	1.017880288	0.719815501	1.392439
1	0.914623179	0.637949266	1.097554057
1.5	0.8937672	0.620350335	1.025412022
2	0.886401958	0.614124014	0.992703752
W_{max}/h	[0/45/-45/90/0/45/-45/90]		
	Boundary Condition		
	SSSS	SCSC	CCCC
0.5	0.949228308	0.857224276	1.262529587
1	0.881421544	0.761390319	1.053566689
1.5	0.868473041	0.740984643	1.000178638
2	0.863880721	0.733772977	0.975261178

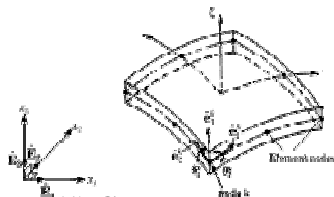


Figure (1) General curved shell elements

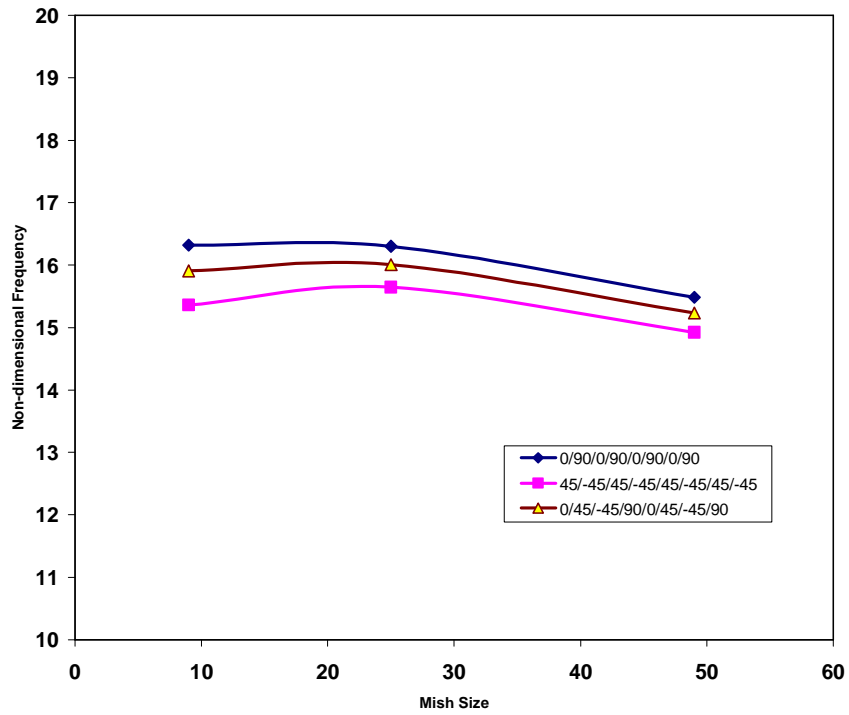


Figure (2) Convergence study of non-dimensional frequency for square shell having SSSS boundary condition with different stacking sequences

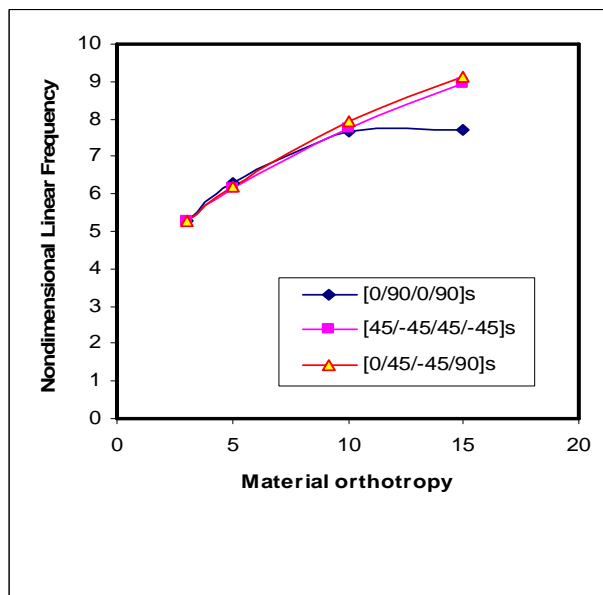


Figure (3) Effect of material orthotropy on linear free vibration of laminated cylindrical shell

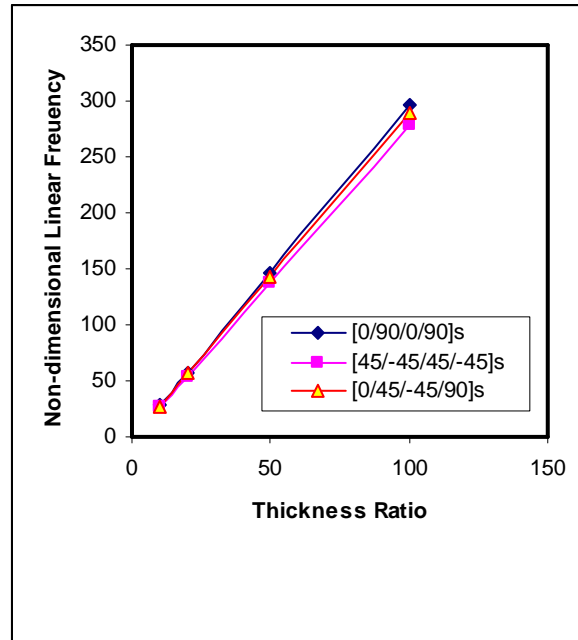


Figure (4) Effect of different thickness ratio on frequency ratio of laminated cylindrical shell

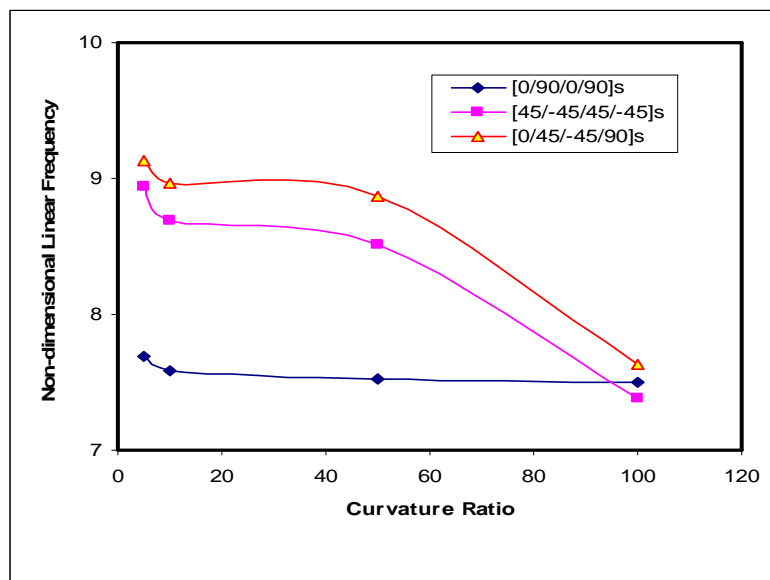


Figure (5) The effect of curvature ratios with the non-dimensional linear frequency

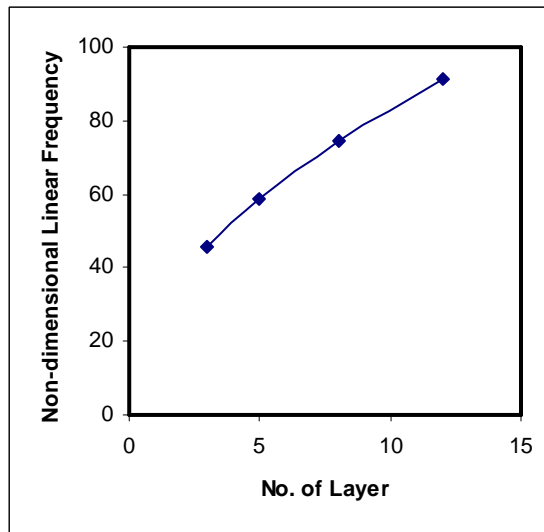


Figure (6) The effect of number of layers on the non-dimensional linear frequency for $[0/90]_n$

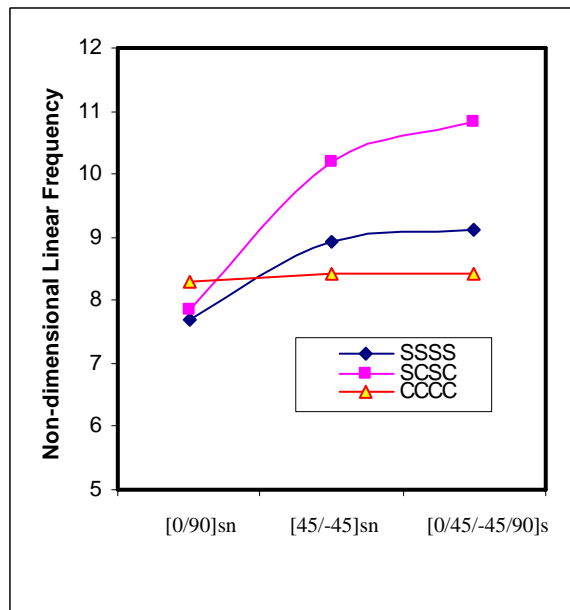


Figure (7) Effect on variable boundary conditions on the non-dimensional linear frequency

Appendix (A)

$$\{\varepsilon\} = \begin{Bmatrix} \varepsilon_{\alpha,\alpha} \\ \varepsilon_{\beta,\beta} \\ \gamma_{\alpha,\beta} \\ \gamma_{\alpha,\zeta} \\ \gamma_{\beta,\zeta} \end{Bmatrix} = \begin{Bmatrix} \left(\frac{\partial \bar{u}}{\partial \alpha} + \frac{\bar{w}}{R_1} \right) \\ \left(\frac{\partial \bar{v}}{\partial \beta} + \frac{\bar{w}}{R_2} \right) \\ \left(\frac{\partial \bar{u}}{\partial \beta} + \frac{\partial \bar{v}}{\partial \alpha} \right) \\ \frac{\partial \bar{u}}{\partial \zeta} + \left(\frac{\partial \bar{w}}{\partial \alpha} - \frac{\bar{u}}{R_1} \right) \\ \frac{\partial \bar{v}}{\partial \zeta} + \left(\frac{\partial \bar{w}}{\partial \beta} - \frac{\bar{v}}{R_2} \right) \end{Bmatrix} + \frac{1}{2} \left\{ 2 \left[\begin{aligned} & \left[\left(\frac{\partial \bar{u}}{\partial \alpha} + \frac{\bar{w}}{R_1} \right)^2 + \left(\frac{\partial \bar{v}}{\partial \alpha} \right)^2 + \left(\frac{\partial \bar{w}}{\partial \alpha} - \frac{\bar{u}}{R_1} \right)^2 \right] \\ & \left[\left(\frac{\partial \bar{v}}{\partial \beta} + \frac{\bar{w}}{R_2} \right)^2 + \left(\frac{\partial \bar{u}}{\partial \beta} \right)^2 + \left(\frac{\partial \bar{w}}{\partial \beta} - \frac{\bar{v}}{R_2} \right)^2 \right] \\ & \left[\left(\frac{\partial \bar{u}}{\partial \alpha} + \frac{\bar{w}}{R_1} \right) \left(\frac{\partial \bar{u}}{\partial \beta} \right) + \left(\frac{\partial \bar{v}}{\partial \alpha} + \frac{\bar{w}}{R_2} \right) \left(\frac{\partial \bar{v}}{\partial \alpha} \right) + \left(\frac{\partial \bar{w}}{\partial \alpha} - \frac{\bar{u}}{R_1} \right) \left(\frac{\partial \bar{w}}{\partial \beta} - \frac{\bar{v}}{R_2} \right) \right] \end{aligned} \right\} \\ \left\{ 2 \left[\begin{aligned} & \left[\left(\frac{\partial \bar{u}}{\partial \alpha} + \frac{\bar{w}}{R_1} \right) \left(\frac{\partial \bar{u}}{\partial \zeta} \right) + \left(\frac{\partial \bar{v}}{\partial \alpha} \right) \left(\frac{\partial \bar{v}}{\partial \zeta} \right) + \left(\frac{\partial \bar{w}}{\partial \alpha} - \frac{\bar{u}}{R_1} \right) \left(\frac{\partial \bar{w}}{\partial \zeta} \right) \right] \right. \right. \\ & \left. \left. 2 \left[\begin{aligned} & \left(\frac{\partial \bar{v}}{\partial \beta} + \frac{\bar{w}}{R_2} \right) \left(\frac{\partial \bar{v}}{\partial \zeta} \right) + \left(\frac{\partial \bar{u}}{\partial \beta} \right) \left(\frac{\partial \bar{u}}{\partial \zeta} \right) + \left(\frac{\partial \bar{w}}{\partial \beta} - \frac{\bar{v}}{R_2} \right) \left(\frac{\partial \bar{w}}{\partial \zeta} \right) \right] \right] \right\} \end{Bmatrix}$$

Or $\{\varepsilon\} = \{\varepsilon_L\} + \{\varepsilon_{NL}\}$

(2)

Where $\{\varepsilon_L\}$ and $\{\varepsilon_{NL}\}$ are the linear and nonlinear strain vectors respectively.

$$\{\varepsilon_L\} + \{\varepsilon_{NL}\} = \begin{Bmatrix} \varepsilon_1^0 \\ \varepsilon_2^0 \\ \varepsilon_6^0 \\ \varepsilon_5^0 \\ \varepsilon_4^0 \end{Bmatrix} + \frac{1}{2} \begin{Bmatrix} \varepsilon_1^4 \\ \varepsilon_2^4 \\ 2\varepsilon_6^4 \\ 2\varepsilon_5^4 \\ 2\varepsilon_4^4 \end{Bmatrix} + \zeta \begin{Bmatrix} \chi_1^1 \\ \chi_2^1 \\ \chi_6^1 \\ \chi_5^1 \\ \chi_4^1 \end{Bmatrix} + \frac{1}{2} \begin{Bmatrix} \chi_1^5 \\ \chi_2^5 \\ 2\chi_6^5 \\ 2\chi_5^5 \\ 2\chi_4^5 \end{Bmatrix} + \zeta^2 \begin{Bmatrix} \chi_1^2 \\ \chi_2^2 \\ \chi_6^2 \\ \chi_5^2 \\ \chi_4^2 \end{Bmatrix} + \frac{1}{2} \begin{Bmatrix} \chi_1^6 \\ \chi_2^6 \\ 2\chi_6^6 \\ 2\chi_5^6 \\ 2\chi_4^6 \end{Bmatrix}$$

$$+ \zeta^3 \begin{Bmatrix} \chi_1^3 \\ \chi_2^3 \\ \chi_5^3 \\ \chi_4^3 \end{Bmatrix} + \frac{1}{2} \begin{Bmatrix} \chi_1^7 \\ \chi_2^7 \\ 2\chi_6^7 \\ 2\chi_4^7 \end{Bmatrix} + \zeta^4 \begin{Bmatrix} \chi_1^8 \\ \chi_2^8 \\ 2\chi_6^8 \\ 2\chi_4^8 \end{Bmatrix} + \zeta^5 \begin{Bmatrix} \chi_1^9 \\ \chi_2^9 \\ 2\chi_6^9 \\ 2\chi_4^9 \end{Bmatrix} + \zeta^6 \begin{Bmatrix} \chi_1^{10} \\ \chi_2^{10} \\ 2\chi_6^{10} \\ 0 \\ 0 \end{Bmatrix} \tag{3}$$

$$\{\varepsilon\} = \{\varepsilon_L\} + \{\varepsilon_{NL}\} = [S]_L \{\bar{\varepsilon}\}_L + \frac{1}{2} [S]_{NL} \{\bar{\varepsilon}\}_{NL}$$

(4)

Where

$$\begin{aligned}
 \{\bar{\varepsilon}\}_L &= \{\varepsilon_1^0 \quad \varepsilon_2^0 \quad \varepsilon_6^0 \quad \varepsilon_5^0 \quad \varepsilon_4^0 \quad \chi_1^1 \quad \chi_2^1 \quad \chi_6^1 \quad \chi_5^1 \quad \chi_4^1 \quad \chi_1^2 \quad \chi_2^2 \quad \chi_6^2 \quad \chi_5^2 \quad \chi_4^2 \\
 &\quad \chi_1^3 \quad \chi_2^3 \quad \chi_6^3 \quad \chi_5^3 \quad \chi_4^3\} \\
 \{\bar{\varepsilon}\}_{NL} &= \{\varepsilon_1^4 \quad \varepsilon_2^4 \quad \varepsilon_6^4 \quad \varepsilon_5^4 \quad \varepsilon_4^4 \quad \chi_1^5 \quad \chi_2^5 \quad \chi_6^5 \quad \chi_5^5 \quad \chi_4^5 \quad \chi_1^6 \quad \chi_2^6 \quad \chi_6^6 \quad \chi_5^6 \quad \chi_4^6 \\
 &\quad \chi_1^7 \quad \chi_2^7 \quad \chi_6^7 \quad \chi_5^7 \quad \chi_4^7 \quad \chi_1^8 \quad \chi_2^8 \quad \chi_6^8 \quad \chi_5^8 \quad \chi_4^8 \quad \chi_1^9 \quad \chi_2^9 \quad \chi_6^9 \quad \chi_5^9 \quad \chi_4^9 \\
 &\quad \chi_1^{10} \quad \chi_2^{10} \quad \chi_6^{10}\}
 \end{aligned}$$

$$\begin{Bmatrix} \sigma_\alpha \\ \sigma_\beta \\ \sigma_{\alpha\beta} \\ \sigma_{\alpha\zeta} \\ \sigma_{\beta\zeta} \end{Bmatrix}^k = \begin{bmatrix} \bar{Q}_{11} & \bar{Q}_{12} & \bar{Q}_{16} & 0 & 0 \\ \bar{Q}_{12} & \bar{Q}_{22} & \bar{Q}_{26} & 0 & 0 \\ \bar{Q}_{16} & \bar{Q}_{26} & \bar{Q}_{66} & 0 & 0 \\ 0 & 0 & 0 & \bar{Q}_{55} & \bar{Q}_{45} \\ 0 & 0 & 0 & \bar{Q}_{45} & \bar{Q}_{44} \end{bmatrix}^k \begin{Bmatrix} \varepsilon_1 \\ \varepsilon_2 \\ \varepsilon_6 \\ \varepsilon_5 \\ \varepsilon_4 \end{Bmatrix}^k$$

(5)

Where :

$$\begin{aligned}
 \bar{Q}_{11} &= Q_{11} \cdot \cos^4 \vartheta + 2(Q_{12} + 2Q_{66}) \cdot \sin^2 \vartheta \cdot \cos^2 \vartheta + Q_{22} \cdot \sin^4 \vartheta \\
 \bar{Q}_{12} &= (Q_{11} + Q_{22} - 4Q_{66}) \cdot \sin^2 \vartheta \cdot \cos^2 \vartheta + Q_{11} (\cos^4 \vartheta + \sin^4 \vartheta) \\
 \bar{Q}_{22} &= Q_{11} \sin^4 \vartheta + 2(Q_{12} + 2Q_{66}) \sin^2 \vartheta \cdot \cos^2 \vartheta + Q_{22} \cos^4 \vartheta \\
 \bar{Q}_{16} &= (Q_{11} - Q_{12} - 2Q_{66}) \sin \vartheta \cdot \cos^3 \vartheta + (Q_{12} - Q_{22} + 2Q_{66}) \sin^3 \vartheta \cdot \cos \vartheta \\
 \bar{Q}_{26} &= (Q_{11} - Q_{12} - 2Q_{66}) \sin^3 \vartheta \cdot \cos \vartheta + (Q_{12} - Q_{22} + 2Q_{66}) \sin \vartheta \cdot \cos^3 \vartheta
 \end{aligned}$$

$$\begin{aligned} \bar{Q}_{66} &= (Q_{11} + Q_{22} - 2Q_{12} - 2Q_{66}) \sin^2 \vartheta \cdot \cos^2 \vartheta + Q_{66} (\sin^4 \vartheta + \cos^4 \vartheta) \\ \bar{Q}_{44} &= Q_{44} \cos^2 \vartheta + Q_{55} \sin^2 \vartheta \\ \bar{Q}_{45} &= (Q_{55} - Q_{44}) \cos \vartheta \cdot \sin \vartheta \\ \bar{Q}_{55} &= Q_{55} \cos^2 \vartheta + Q_{44} \sin^2 \vartheta \end{aligned}$$

$$\begin{aligned} U &= \frac{1}{2} \int_V \{ \varepsilon_L + \varepsilon_{NL} \}_i^T [\bar{Q}] \{ \varepsilon_L + \varepsilon_{NL} \}_i dV \\ &= \frac{1}{2} \int \left(\{ \varepsilon_L \}_i^T [D_1] \{ \varepsilon_L \}_i + \frac{1}{2} \{ \varepsilon_L \}_i^T [D_2] \{ \varepsilon_{NL} \}_i + \frac{1}{2} \{ \varepsilon_{NL} \}_i^T [D_3] \{ \varepsilon_L \}_i + \frac{1}{4} \{ \varepsilon_{NL} \}_i^T [D_4] \{ \varepsilon_{NL} \}_i \right) dA \end{aligned}$$

(7)

Where :

$$\begin{aligned} [D_1] &= \sum_{k=1}^N \int_{\zeta_{k-1}}^{\zeta_k} [\mathcal{S}]_L^T [\bar{Q}] [\mathcal{S}]_L d\zeta \\ [D_2] &= \sum_{k=1}^N \int_{\zeta_{k-1}}^{\zeta_k} [\mathcal{S}]_L^T [\bar{Q}] [\mathcal{S}]_{NL} d\zeta \\ [D_3] &= \sum_{k=1}^N \int_{\zeta_{k-1}}^{\zeta_k} [\mathcal{S}]_{NL}^T [\bar{Q}] [\mathcal{S}]_L d\zeta \\ [D_4] &= \sum_{k=1}^N \int_{\zeta_{k-1}}^{\zeta_k} [\mathcal{S}]_{NL}^T [\bar{Q}] [\mathcal{S}]_{NL} d\zeta \end{aligned}$$

Where : N is the numbers of layers

$$\{\bar{\delta}\}_i = \begin{Bmatrix} \bar{u} \\ \bar{v} \\ \bar{w} \end{Bmatrix} = \begin{bmatrix} 1 & 0 & 0 & \zeta & 0 & \zeta^2 & 0 & \zeta^3 & 0 \\ 0 & 1 & 0 & 0 & \zeta & 0 & \zeta^2 & 0 & \zeta^3 \\ 0 & 0 & 1 & 0 & 0 & 0 & 0 & 0 & 0 \end{bmatrix} \begin{Bmatrix} \dot{u} \\ \dot{v} \\ \dot{w} \\ \dot{\phi}_1 \\ \dot{\phi}_2 \\ \dot{\psi}_1 \\ \dot{\psi}_2 \\ \dot{\theta}_1 \\ \dot{\theta}_2 \end{Bmatrix} = [f]\{\dot{\delta}\} \tag{9}$$

Where, $[f]$ is the function of the thickness coordinate.

$$\begin{Bmatrix} x \\ y \\ z \end{Bmatrix} = \sum N_i(\alpha, \beta) \frac{(1+\zeta)}{2} \begin{Bmatrix} x_i \\ y_i \\ z_i \end{Bmatrix}_{Top} + \sum N_i(\alpha, \beta) \frac{(1-\zeta)}{2} \begin{Bmatrix} x_i \\ y_i \\ z_i \end{Bmatrix}_{bottom} \tag{11}$$

Where (N) is the Lagrangian interpolation function and (i) is the node number.

$$U = \frac{1}{2} \int_A \left([B_L]_i^T \{\delta\}_i^T [D_1][B_L]_i \{\delta\}_i + \frac{1}{2} [B_L]_i^T \{\delta\}_i^T [D_2][B_{NL}]_i \{\delta\}_i + \frac{1}{2} [B_{NL}]_i^T \{\delta\}_i^T [D_3][B_L]_i \{\delta\}_i + \frac{1}{4} [B_{NL}]_i^T \{\delta\}_i^T [D_4][B_{NL}]_i \{\delta\}_i \right) dA \tag{13}$$

Where $[B_{NL}]_i = [A]_i [G]_i$, $[A]_{33 \times 27}$ is function to the displacements and $[G]_{27 \times 9}$ is the product form of differential operator and shape function in the nonlinear strain terms. $[B_L]_{20 \times 9}$ is the product form of the differential operator and nodal interpolation function in the linear terms.